INVITED PAPER *Special Section on Opto-electronics and Communications for Future Optical Network*

Magneto-Optical Microring Switch Based on Amorphous Silicon-on-Garnet Platform for Photonic Integrated Circuits

Toshiya MURAI[†a)], ***Nonmember***, **Yuya SHOJI**[†,††], ***Member***, **Nobuhiko NISHIYAMA**[†,††], ***Senior Member***, ***and*** **Tetsuya MIZUMOTO**[†], ***Fellow***

SUMMARY Magneto-optical (MO) switches operate with a dynamically applied magnetic field. The MO devices presented in this paper consist of microring resonators (MRRs) fabricated on amorphous silicon-on-garnet platform. Two types of MO switches with MRRs were developed. In the first type, the switching state is controlled by an external magnetic field component included in the device. By combination of MO and thermo–optic effects, wavelength tunable operation is possible without any additional heater, and broadband switching is achievable. The other type of switch is a self-holding optical switch integrated with an FeCoB thin-film magnet. The switching state is driven by the remanence of the integrated thin-film magnet, and the state is maintained without any power supply.

key words: *photonic integrated circuits, magneto-optical, material, microring resonator, optical switch*

1. Introduction

The data traffic in datacenters and across optic fiber networks has grown significantly, driving development of high-speed and low-power photonic integrated circuits (PICs) for optical interconnects and optical transceivers. The rapid rise in PIC technology has also spurred research interest in optical computing challenges, such as optical neural networks, which seemed impossible to realize only a decade ago [1], [2]. However, a practical optical computing device requires more power efficient PICs. To meet this demand, photonic devices have been combined with nonvolatile switching materials, such as phase-change material, which has been widely studied recently [3], [4]. The nonvolatile optical switch could reduce power consumption of PICs drastically because it would require no power to maintain its switching state. Nonvolatile optical memory is also sought, but it remains a challenging device for optical signal processing.

We believe that integration of photonic devices with magneto-optical (MO) materials is a pathway to nonvolatile optical switches and optical memories in PICs. MO materials exhibit unique optical features such as optical nonreciprocity and magnetic nonvolatility. The interaction of light with any kind of magnetic medium creates a magneto-optical effect. The reflectivity of a lightwave with a transverse magnetic (TM) polarization that reflects at the surface of MO material is slightly changed by the transverse MO Kerr effect when the magnetization is in-plane and perpendicular to the direction of the incident light. In a planar waveguide system, light may experiences a nonreciprocal phase shift (NPS), i.e., a phase shift dependent on the direction of propagation or magnetization. Employing an NPS effect in a static magnetic field yielded an optical isolator [5], [6] and an optical circulator [7], [8]. When the magnetic field is controlled dynamically, an optical switch [9] and a modulator are obtained.

An MO garnet is a ferrimagnetic material with a large Faraday rotation coefficient and low optical absorption at telecommunication wavelengths. On-chip optical devices with cerium-substituted-yttrium iron garnet (Ce:YIG) have been widely studied. MO devices with Ce:YIG have been obtained by heterogeneous integration of a single crystal garnet using either direct bonding or adhesive bonding [10], or direct deposition of polycrystalline films by pulsed laser deposition or sputtering methods [11], [12]. The bonding technique, which can be performed at relatively low temperature (∼200°C), involves growing a single-crystalline Ce:YIG on a lattice matched gadolinium gallium garnet (GGG) substrate, thus producing Ce:YIG with the largest possible Faraday rotation coefficient. However, additional fabrication or processing after bonding is challenging. Direct deposition can match the scalability of the device function, but polycrystalline garnet requires high temperature (∼900°C) for crystal growth and has smaller Faraday rotation relative to single-crystal Ce:YIG, owing to inferior crystallinity.

In this paper, we describe our recent progress on microring MO switches dynamically controlled by a magnetic field. The devices were fabricated based on the amorphous silicon (a-Si:H)-on-garnet platform. On this platform, the single crystal Ce:YIG with large Faraday rotation coefficient of −4500°/cm is used as a lower cladding layer, and functional structures can be added onto the waveguides relatively easily. The numerical design and fabrication technique of the a-Si:H waveguide on MO garnet are initially described, followed by the fabrication of an MO microring switch and analysis of the switching characteristics obtained by controlling a current-induced magnetic field. A self-holding MO switch integrated with a thin-film magnet

Manuscript received December 26, 2019.
Manuscript revised April 15, 2020.
Manuscript publicized June 5, 2020.

[†]The authors are with Department of Electrical and Electronic Engineering, Tokyo Institute of Technology, Tokyo, 152–8552 Japan.
[††]The authors are with Laboratory for Future Interdisciplinary Research of Science and Technology (FIRST), Tokyo Institute of Technology, Tokyo, 152–8552 Japan.
a) E-mail: murai.t.ae@m.titech.ac.jp

DOI: 10.1587/transele.2019OCP0003

is then demonstrated. This switch is controlled by the remanent magnetization of the integrated thin-film magnet; thus, it does not consume electrical energy to maintain the switching state. The future perspective of the on-chip MO device is discussed at the end of the paper.

2. Magneto-Optical Effect in an a-Si:H on Garnet Waveguide

2.1 Design

A schematic of the cross section of the amorphous silicon-on-garnet waveguide is shown in Fig. 1. The structure of the waveguide was designed to maximize the magneto-optical effect under investigation, in this case a nonreciprocal phase shift (NPS) effect. A $CeY_2Fe_5O_{12}$ (Ce:YIG) crystal of thickness 500 nm was epitaxially grown on a (111)-oriented (Ca, Mg, Zr)-substituted GGG substrate (SGGG). An a-Si:H waveguide was formed on the Ce:YIG layer, including a 10 nm SiO_2 interlayer to prevent diffusion of Fe from Ce:YIG into the a-Si:H, thereby increasing the absorption loss. The NPS is available only for the fundamental TM mode as the magneto-optical cladding layer is under the a-Si:H waveguide. Hence, the following simulations and experiments are performed under TM.

The change of propagation constant induced by the NPS was analyzed using the two-dimensional finite element method (FEM), with the parameters in Table 1 as inputs. Figure 2 shows the NPS $\Delta\beta$ for different heights and widths of the a-Si:H waveguide [9]. The dotted lines indicate radiated modes that do not propagate in the waveguide. The sharp dips centered at a width of ~0.8 μm are induced by the undesirable excitation of hybrid modes of TM_0 and TE_1. Waveguide widths in this range were excluded from the design. The maximized NPS is almost insensitive to changes in the waveguide width when the width is varied within a range close to 1 μm. Therefore, waveguide width $w_{a\text{-}Si}$ = 1 μm was adopted for the design. The waveguide height was selected by calculating NPS and absorption loss values for Ce:YIG at different waveguide heights with $w_{a\text{-}Si}$ = 1 μm. The results are shown in Fig. 3. The NPS is maximized at waveguide heights between 200 and 210 nm; however, the absorption loss of Ce:YIG is also high in this range, indicating that a tradeoff may be warranted. Considering both the NPS and the absorption loss, a waveguide geometry of $w_{a\text{-}Si}$ = 1 μm and $h_{a\text{-}Si}$ = 220 nm, with NPS $\Delta\beta$ = ~5.3

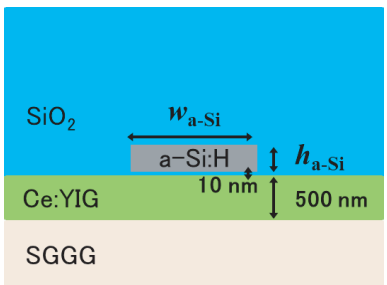

Fig. 1 Schematic structure of a-Si:H/Ce:YIG waveguide for simulation with FEM.

Table 1 Parameters for simulation of finite element method.

Parameter	Quantity	Value
$n_{a\text{-}Si:H}$	Refractive index of a-Si:H	3.48
n_{SiO2}	Refractive index of SiO_2	1.44
$n_{Ce:YIG}$	Refractive index of Ce:YIG	2.22
n_{SGGG}	Refractive index of SGGG	1.94
$\alpha_{Ce:YIG}$	Extinction coefficient of Ce:YIG	1.22×10^{-4}
Θ_F	Faraday rotation coefficient of Ce:YIG	-4500 °/cm
λ	Wavelength	1550 nm

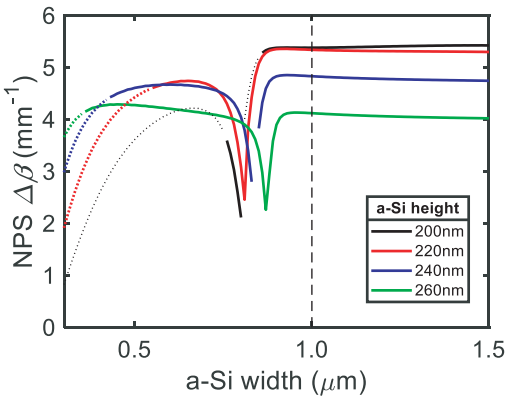

Fig. 2 Calculated NPS of the a-Si:H/Ce:YIG waveguide.

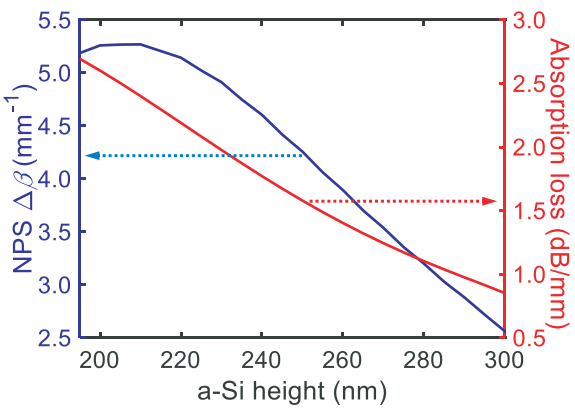

Fig. 3 Calculated NPS and absorption loss of the a-Si:H/Ce:YIG waveguide with width 1 μm.

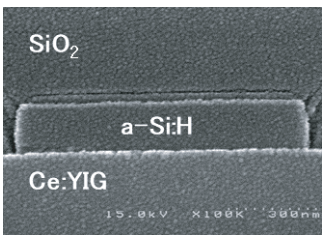

Fig. 4 SEM image of the amorphous silicon-on garnet waveguide.

mm^{-1}, was chosen.

2.2 Fabrication

Fabrication of the amorphous silicon-on-garnet waveguide began with growth of a 500 nm Ce:YIG single crystal on an SGGG substrate by an RF sputtering method. This was followed by addition of a 10 nm SiO_2 interlayer, and then deposition of a 220 nm a-Si:H waveguide from SiH_4 gas and Ar plasma, by plasma-enhanced chemical vapor deposition (PE-CVD) at 300°C. The a-Si:H waveguides were formed using 100 keV electron beam lithography and reactive ion etching with SF_6 gas. An SiO_2 upper cladding layer was deposited by PE-CVD as the final step. Figure 4 is a scanning electron microscopic (SEM) image of the cross-section of the fabricated waveguide.

3. Switching Operation Controlled by Current-Induced Magnetic Field

A race track-shaped microring switch (MRR) was fabricated containing waveguides with curved sections of radius 50 μm and straight sections of length 9 μm, as shown in Fig. 5. A 700 nm Cr/Au electromagnetic coil was formed on the fabricated MRR by a lift-off procedure, as the source of current-induced magnetic field applied to the Ce:YIG. Figure 6 is a cross-sectional schematic of the MRR device. MO effects were investigated with both a static and a temporally varying magnetic field, and a wavelength-tunable operation was developed. All measurements were performed on a stage with temperature maintained at 20°C by a thermoelectric cooler. The TM polarized light was coupled to the cleaved facet of the waveguide through a lens-tipped fiber.

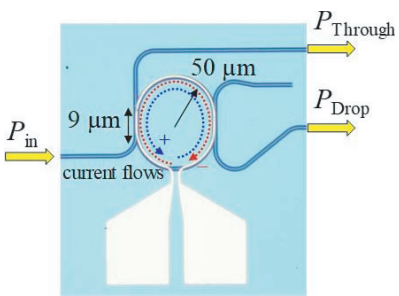

Fig. 5 Microscopic image of the fabricated MO microring switch (MRR).

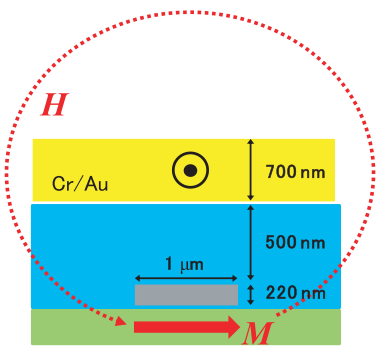

Fig. 6 Schematic image of the cross-sectional structure of the a-Si:H/Ce:YIG MRR device.

3.1 Static Operation

Output from the MRR was measured as transmitted spectra using an amplified spontaneous emission (ASE) light source and a spectrum analyzer. The electromagnetic coil was connected to a variable voltage source through microprobes. For static operation, a DC electric current of 62 mA was applied to the electromagnetic coil, in both the clockwise (CW) and the counterclockwise (CCW) directions. The corresponding transmitted spectra are shown in Fig. 7.

Various directions of the in-plane magnetic field transverse to the light propagation were induced in the Ce:YIG. Resonant wavelength shifts that were dependent on the direction of the current flow were observed at both the through and drop ports. A thermo-optic (TO) redshift of the resonant wavelengths, which was independent of the current direction, was also observed as a result of Joule heating of the coil. The extinction ratios of switching at the through and drop ports were ~10 dB and ~5 dB at 1559.16 nm, re-

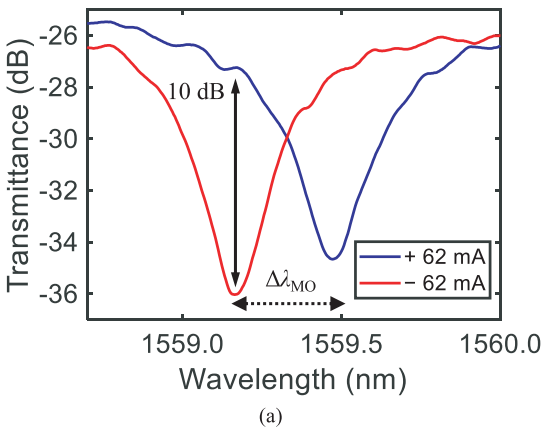

(a)

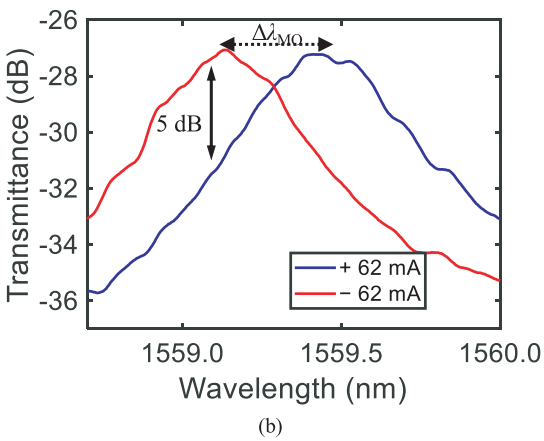

(b)

Fig. 7 Transmitted spectra from the MO switch controlled by a static external magnetic field at (a) the through port and (b) the drop port.

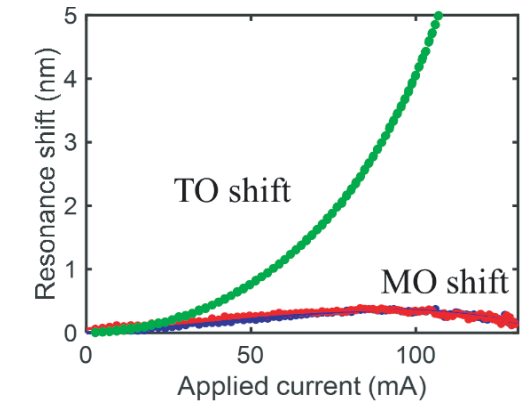

(a)

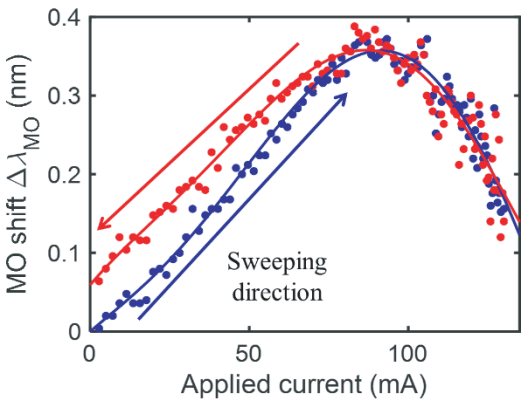

(b)

Fig. 8 (a) MO and TO shifts for each applied current (b) MO shifts extracted from (a).

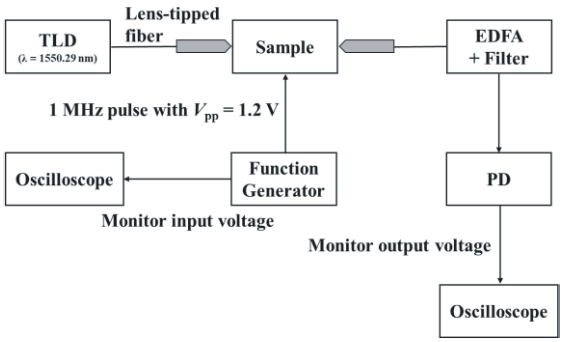

Fig. 9 The measurement setup for the time-domain measurement of the MO switch.

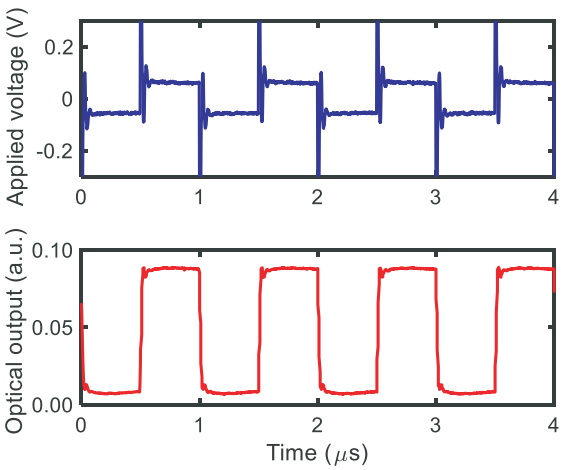

Fig. 10 Time base response of MO device to a 1 MHz rectangle wave voltage. Applied voltage was measured by oscilloscope. Optical output was measured by a photodiode connected to an oscilloscope.

spectively. The Q-factor is ~3,000. Considering input and output fiber waveguide coupling losses of ~25 dB, the insertion loss was estimated to be ~2 dB at the through port. The resistance of the coil was close to ~5 Ω; hence, the power consumption was ~20 mW, which is lower than the power consumption previously reported for a microring MO device fabricated by the bonding technique [7]. In the present study, the electromagnetic coil is closer to the MO material and the magnetic field is more efficiently applied to the Ce:YIG. The thickness of the Au microstrip was limited to 700 nm in our in-house fabrication procedure, but increasing the thickness improves power consumption by several milliwatts. Therefore, the extinction ratio of both ports can be improved by using cascading double microrings.

The resonance shifts at various applied DC currents were measured by increasing the current value from 0 to 130 mA and decreasing from 130 to 0 mA. The MO effect is the nonreciprocal effect, hence dependent on the magnetization direction. The TO redshift is a reciprocal effect independent of the magnetization direction. Therefore, each effect was easily distinguished. Figure 8 (a) shows both the MO and TO phase shifts. The TO shift increased quadratically with applied current. Figure 8 (b) shows the MO results in more detail. The MO shift reaches a maximum at ~80 mA, and then decreases with increasing current. This phenomenon results from the temperature dependence of the Faraday rotation coefficient of Ce:YIG: $d\Theta_F/dT$ = +44°/cm/K [13] and the temperature rise in the device due to Joule heating at higher current. After reducing the current to 0 mA, an MO shift is detectable in accordance with the remanent magnetization of Ce:YIG.

3.2 Temporal Operation

The ASE light source was replaced by a tunable laser diode (TLD) with output wavelength 1550.29 nm. The measurement setup is shown in Fig. 9. A rectangular wave voltage with a frequency of 1 MHz and 50% duty cycle was fed by a function generator to dynamically control the Ce:YIG magnetization. The applied voltage was monitored, and the time base optical output at the through port was measured using a photodiode coupled to a sampling oscilloscope. Figure 10 shows the signals obtained for both.

The optical output power follows the applied voltage; however, the rise and fall cycle of the optical response was

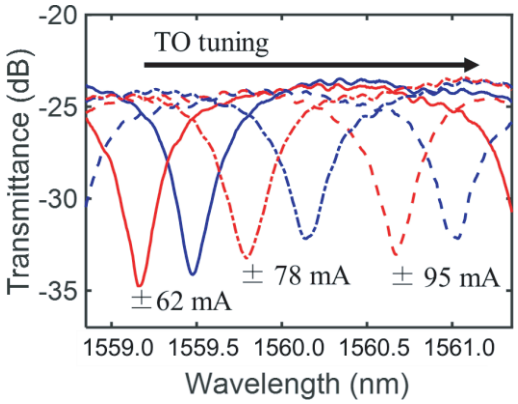

Fig. 11 Wavelength tunable operation of the MO switch by TO tuning.

found to be restricted to a minimum of 20 ns. This corresponds to a maximum response frequency of 50 MHz, even though the reversal of magnetization takes place over a few picoseconds [14]. The spike and the oscillation of the applied voltage (Fig. 10) caused by the inductance of the coil are responsible for limiting the response frequency of the device. The small resistance of 5 Ω suppressed the effective voltage applied by the function generator for 50 Ω systems. Optimization of the coil design such that it is impedance matching would enable the switch to operate at frequencies over a few tens of GHz, i.e., a cycle time of the order of 50-100 picoseconds. In the fabricated device, the bandwidth calculated from the 3 dB width was ~20 GHz at the through port. Therefore, the data rate might be limited to ~40 Gbps.

3.3 Wavelength-Tunable Operation

Combining the TO and MO effects enables tuning of the operational wavelength. Increasing the DC current from 60 to 100 mA produced a significant phase shift attributable to the TO effect (Fig. 8 (a)). Thus, the operational output wavelength is tunable, as demonstrated in Fig. 11, and broadband switching over the full fiber-optic C band (1530-1565 nm) is possible because the TO shift of the device is significantly larger than its free-spectral range (~2.2 nm). This tuning mechanism is also applicable to the operation of a wavelength locking controller, which maintains the resonant wavelength against ambient temperature change without additional heater.

4. Self-Holding Switch Controlled by Remanent Magnetization of Thin-Film Magnet

In Fig. 8 (b), a small phase shift is present after the current is switched off, owing to a weak remanent magnetization of Ce:YIG. Therefore, combination of Ce:YIG and a magnetic material with strong remanence will enable the use of the device as a nonvolatile optical switch [15]. This can be achieved by forming a thin-film magnet on the waveguide to maintain a magnetic field by remanent magnetization when the coil is not operating. The magnetization of the thin-film

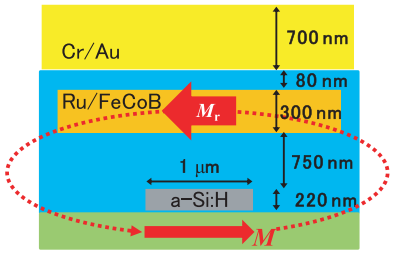

Fig. 12 Schematic image of the cross-sectional structure of the self-holding MO switch.

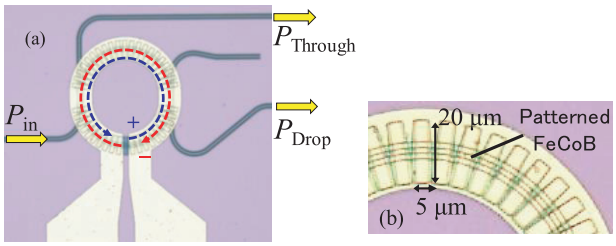

Fig. 13 Microscopic image of the MO microring switch, (a) image of the device, and (b) the patterned FeCoB thin-film magnet.

magnet is controlled by the magnetic field induced by a current in the electromagnetic coil formed above. The MO effect in the Ce:YIG layer is self-holding (i.e., fixed) at the level determined by the remanence in the absence of a power supply. A schematic of the cross section of the self-holding MO phase shifter is depicted in Fig. 12.

Based on our previous work, the MRR switch was fabricated on garnet substrate. Using an RF facing target sputtering method, 300 nm FeCoB magnet layer and 10 nm Ru buffer layer were integrated on a 750 nm SiO_2 cladding layer, which was enough thickness so as not to bring about a notable optical absorption. FeCoB is a soft magnetic material with large remanent magnetization and low coercive force. The thin-film magnet was patterned using a lift-off procedure to form an array of 20 μm × 5 μm stripes. An 80 nm layer of SiO_2 was then deposited, followed by an Cr/Au electromagnetic coil of thickness 700 nm, to flip the magnetization of FeCoB by a current-induced magnetic field. Figure 13 (a) is an image of the fabricated device. The magnetization of FeCoB was aligned along the long axis of the stripes, which is transverse to the direction of light propagation. Therefore, the magnetization of FeCoB is applied to the radial direction of the microring. Figure 13 (b) is the microscopic image of the patterned magnet.

4.1 Static Operation

Operation of the device in self-holding mode (constant MO effect, no power supply) is demonstrated by controlling the direction of remanent magnetization of FeCoB. The characteristics of the device in a static magnetic field were initially established. A 500 mA current was applied to the coil in the CCW direction to magnetize FeCoB along the radial direction of the MRR. Transmission spectra were mea-

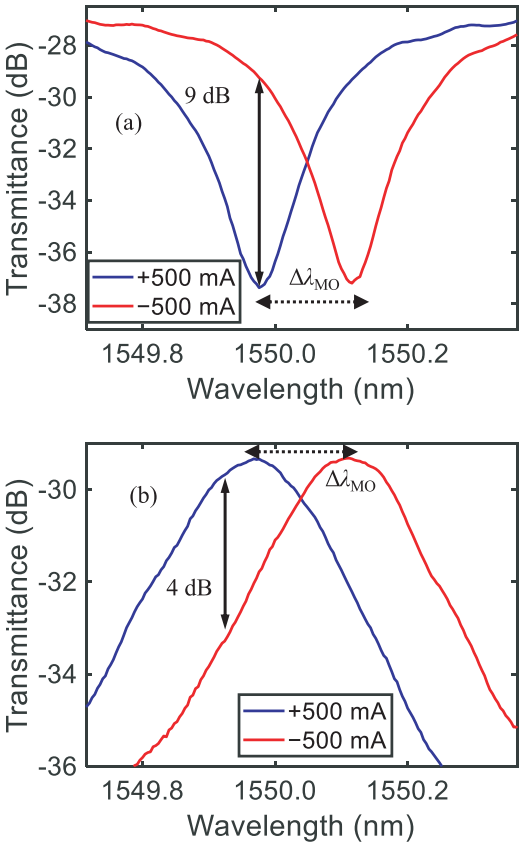

Fig. 14 Transmitted spectra of the MO switch controlled by remanent magnetization of thin-film magnet at (a) the through port and (b) the drop port.

sured several seconds after switching off the current, using the ASE light source with TM mode polarization. The direction of current flow was then applied to the coil in the reverse (CW) direction, and transmitted spectra measured. Figure 14 shows the spectra obtained at the through and drop ports. The resonant wavelength was shifted to longer or shorter wavelength as a result of the MO phase shift induced by remanence of FeCoB in the opposite direction. The extinction ratios of the switching at the through and drop ports were ~9 dB and ~4 dB at a wavelength of 1549.95 nm. The Q-factor is ~5,000. The wavelength shift was ~0.14 nm. This was one fourth of the calculated value owing to the magnetization of Ce:YIG not attaining full saturation. Optimization of FeCoB position and film thickness to provide larger magnetization improves the phase shift.

4.2 Temporal Operation

The self-holding behavior of the MO switch was measured over time to verify the effect. The device was illuminated with continuous light of wavelength 1550.1 nm, and a pulsed voltage of width 1 μs, amplitude V_{pp} = ~±0.5 V, and frequency 10 kHz was applied to the electromagnetic coil using a function generator. The voltage polarity was flipped periodically. The optical output was detected at the through

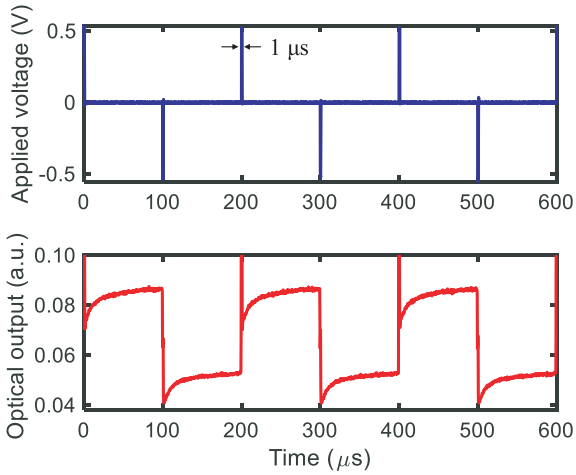

Fig. 15 Measured time base response of MO switch to a pulsed current with a 1 μs width pulsed voltage changing its sign alternately with a repetition rate of 10 kHz.

port by a photodetector with an electrical gain amplifier and observed by a sampling oscilloscope.

Figure 15 shows the temporal response of the optical output. The output alternated between high and low response with the reversal of direction of flow of each current pulse. At 10 kHz, a 1 μs pulsed voltage of +0.5 or −0.5 V was delivered every 100 μs, with 0 V maintained during the 99 μs dwell time. Figure 15 demonstrates that optical power output was maintained during each dwell time. The slow drift after the switching is attributed to thermal relaxation due to Joule heating. Nonvolatile optical devices using a phase-change material have generally been limited to below 10,000 re-writes due to thermally induced material degradation. By contrast, the self-holding MO switch presented in this paper is based on nonvolatile magnetization interacting with light passing through the device material, thus rewriting lifetimes of over 10^6 are possible, dependent only on the long term photostability and permanence of the magnetic properties of the constituent materials.

5. Future Development

An optical memory employing an MO recording scheme has also been envisaged as an application of our amorphous silicon-on-garnet platform. MO recording is used for an MO disk as a removable recording medium [16]. Figure 16 shows a proposed structure and mechanism for MO memory, consisting of a recording/heating layer of FeCoB and a reading layer of Ce:YIG. The optical memory would store 1-bit of optical information as the magnetization direction of the recording layer, which has (at least) two directions, thus would store binary information.

The stored datum could be read out using an MO phase shift and the change of the resonant states of an MRR. Light-to-heat conversion may be employed for the writing operation. This involves optical absorption-induced heating [17]; i.e., when the temperature of a magnetic material increases,

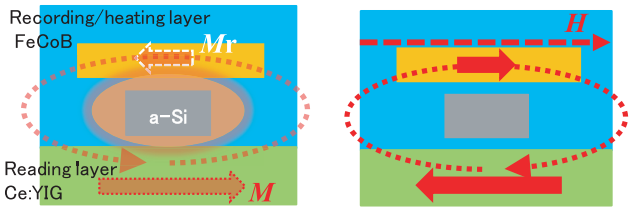

Fig. 16 Schematic image of the proposed MO memory, (a) optical absorption-induced heating and decrease of coercive force and (b) magnetization reversal.

the intensity of the coercive force weakens and its direction is easily reversed along an applied external magnetic field. In our proposed memory, the magnetization of the heating layer is controlled by the electromagnetic field of light in the waveguide. The FeCoB recording/heating layer would be formed with a thinner SiO_2 cladding layer on the waveguide, such that it is exposed to the evanescent field of the waveguide. The FeCoB layer would absorb optical power, unlike the self-holding optical switch in Sect. 4 where FeCoB is deposited on a 750 nm SiO_2 cladding layer, hence not exposed to electromagnetic fields from the waveguide. Consequently, the absorbed light would increase the temperature of FeCoB, reducing its coercive force. The magnetization of FeCoB could then be flipped by a weak external magnetic field, but only when light is injected through the waveguide.

The proposed memory does not require electric power to maintain memory states by virtue of the nonvolatility of the magnetization of the FeCoB recording layer. The multiple-bits memories could be integrated on a large scale in PICs.

6. Conclusion

In this work, we demonstrated magneto-optical microring switches based on an amorphous silicon-on-garnet platform. The device design and fabrication process were described. A switching operation controlled by an external magnetic field generated from the current flowing in an integrated electromagnetic coil was initially presented. Extinction ratios were ~10 dB and ~5 dB at the through and drop ports. Power consumption was ~20 mW. The temporal response of the optical output to an applied 1 MHz rectangle wave voltage was described. Combination of MO and TO effects enabled broadband wavelength tuning. This mechanism is applicable to the wavelength locking controller without any additional heater. Self-holding of the MO effect, controlled by remanent magnetization of an integrated thin-film magnet was then demonstrated. The switching states were changed by reversing the magnetization of FeCoB with an applied current of 500 mA, and the switched states were maintained with zero current. The measured extinction ratios were ~9 dB and ~4 dB at the through and drop ports. To verify the self-holding behavior of the MO switch, the temporal response with a pulsed current of 1-μs width was measured. Finally, an MO memory on a-Si-on-garnet platform was proposed. In future research, a method of controlling magnetization with light should be explored to realize the proposed optical memory device.

Acknowledgments

This study was supported by MIC/SCOPE #162103103; JST Core Research for Evolutional Science and Technology (CREST) #JPMJCR15N6 and #JPMJCR18T4; JSPS KAKENHI #19H02190 and New Energy and Industrial Technology Development Organization (NEDO).

References

[1] K. Kitayama, M. Notomi, M. Naruse, K. Inoue, S. Kawakami, and A. Uchida, "Novel frontier of photonics for data processing-Photonic accelerator," APL Photonics, vol.4, no.9, 2019.
[2] Y. Shen, N.C. Harris, S. Skirlo, M. Prabhu, T. Baehr-Jones, M. Hochberg, X. Sun, S. Zhao, H. Larochelle, D. Englund, and M. Soljačić, "Deep learning with coherent nanophotonic circuits," Nat. Photonics, vol.11, no.7, pp.441–446, 2017.
[3] M. Wuttig, H. Bhaskaran, and T. Taubner, "Phase-change materials for non-volatile photonic applications," Nat. Photonics, vol.11, no.8, pp.465–476, 2017.
[4] P. Xu, J. Zheng, J.K. Doylend, and A. Majumdar, "Low-Loss and Broadband Nonvolatile Phase-Change Directional Coupler Switches," ACS Photonics, vol.6, no.2, pp.553–557, 2019.
[5] Y. Shoji, T. Mizumoto, H. Yokoi, I.-W. Hsieh, and R.M. Osgood, "Magneto-optical isolator with silicon waveguides fabricated by direct bonding," Appl. Phys. Lett., vol.92, no.7, pp.2–5, 2008.
[6] D. Huang, P. Pintus, C. Zhang, Y. Shoji, T. Mizumoto, and J.E. Bowers, "Electrically Driven and Thermally Tunable Integrated Optical Isolators for Silicon Photonics," IEEE J. Sel. Top. Quantum Electron., vol.22, no.6, pp.271–278, Nov. 2016.
[7] D. Huang, P. Pintus, C. Zhang, P. Morton, Y. Shoji, T. Mizumoto, and J.E. Bowers, "Dynamically reconfigurable integrated optical circulators," Optica, vol.4, no.1, pp.23–30, Jan. 2016.
[8] K. Mitsuya, Y. Shoji, and T. Mizumoto, "Demonstration of a Silicon Waveguide Optical Circulator," IEEE Photonics Technol. Lett., vol.25, no.8, pp.721–723, 2013.
[9] T. Murai, Y. Shoji, N. Nishiyama, and T. Mizumoto, "Wavelength-tunable operation of magneto-optical switch consisting of amorphous silicon microring resonator on garnet," Jpn. J. Appl. Phys., vol.58, no.7, 2019.
[10] T. Mizumoto, R. Baets, and J.E. Bowers, "Optical nonreciprocal devices for silicon photonics using wafer-bonded magneto-optical garnet materials," MRS Bull., vol.43, no.6, pp.419–424, 2018.
[11] Y. Zhang, Q. Du, C. Wang, T. Fakhrul, S. Liu, L. Deng, D. Huang, P. Pintus, J. Bowers, C.A. Ross, J. Hu, and L. Bi, "Monolithic integration of broadband optical isolators for polarization-diverse silicon photonics," Optica, vol.6, no.4, p.473, 2019.
[12] L. Bi, J. Hu, P. Jiang, D.H. Kim, G.F. Dionne, L.C. Kimerling, and C.A. Ross, "On-chip optical isolation in monolithically integrated non-reciprocal optical resonators," Nat. Photonics, vol.5, no.12, pp.758–762, 2011.
[13] K. Furuya, T. Nemoto, K. Kato, Y. Shoji, and T. Mizumoto, "Athermal operation of a waveguide optical isolator based on canceling phase deviations in a Mach-Zehnder interferometer," J. Light. Technol., vol.34, no.8, pp.1699–1705, 2016.
[14] I. Tudosa, C. Stamm, A.B. Kashuba, F. King, H.C. Siegmann, J. Stöhr, G. Ju, B. Lu, and D. Weller, "The ultimate speed of magnetic switching in granular recording media," Nature, vol.428, no.6985,

pp.831–833, 2004.
[15] K. Okazeri, K. Muraoka, Y. Shoji, S. Nakagawa, N. Nishiyama, S. Arai, and T. Mizumoto, "Self-Holding Magneto-Optical Switch Integrated With Thin-Film Magnet," IEEE Photonics Technol. Lett., vol.30, no.4, pp.371–374, 2018.
[16] T.W. McDaniel and R. Victora, "Handbook of magneto-optical data recording: materials, subsystems, techniques," Elsevier, 1995.
[17] T. Murai, Y. Shoji, and T. Mizumoto, "Efficient Light-to-Heat Conversion by Optical Absorption of a Metal on an Si Microring Resonator," J. Light. Technol., vol.37, no.10, pp.2223–2231, 2019.

Toshiya Murai received the B.E. and M.E. degrees in electrical and electronic engineering from the Tokyo Institute of Technology, Tokyo, Japan, in 2016 and 2019, respectively. He is currently working toward the Ph.D. degree. His current research interests include silicon photonic devices with magneto-optical material.

Yuya Shoji received the B.E., M.E., and Ph.D. degrees in electrical engineering from the Tokyo Institute of Technology, Tokyo, Japan, in 2003, 2005, and 2008, respectively. He was a Postdoctoral Fellow with the National Institute of Advanced Industrial Science and Technology, Tsukuba, Japan, from 2008 to 2010. He has been an Assistant Professor with the Graduate School of Science and Engineering, Tokyo Institute of Technology, from 2011 to 2014. He is currently an Associate Professor with the Laboratory for Future Interdisciplinary Research of Science and Technology, Tokyo Institute of Technology. His current research interests include device designs and fabrication of magneto-optical devices, silicon nanophotonic devices, and the photonic integrated circuits. He is a member of the Optical Society of America, the Institute of Electronics, Information and Communication Engineers, the Japan Society of Applied Physics, and the Magnetic Society of Japan.

Nobuhiko Nishiyama was born in Yamaguchi Prefecture, Japan, in 1974. He received the B.E., M.E., and Ph.D. degrees from the Tokyo Institute of Technology, Japan, in 1997, 1999, and 2001, respectively. During his Ph.D. work, he demonstrated single-mode 0.98-and 1.1-μm VCSEL arrays with stable polarization using misoriented substrates for high-speed optical networks and MOCVD-grown GaInNAs VCSELs. He joined Corning, Inc., New York, in 2001, and worked with the Semiconductor Technology Research Group. At Corning, he worked on several subjects, including short-wavelength lasers, 1060-nm DFB/DBR lasers, and long-wavelength InP-based VCSELs. Since 2006, he has been an Associate Professor with the Tokyo Institute of Technology. His current main interests include transistor lasers, silicon photonics, III–V silicon hybrid optical devices, and terahertz–optical signal conversions involving optics–electronics–radio integration circuits. Dr. Nishiyama is a member of the Japan Society of Applied Physics (JSAP), IEEE and IEICE. He was the recipient of the Excellent Paper Award from the Institute of Electronics, Information and Communication Engineers (IEICE) of Japan in 2001, the Young Scientists' Prize of the Commendation for Science and Technology from the Minister of Education, Culture, Sports, Science and Technology in 2009, and the Ichimura Prize in Science for Distinguished Achievement in 2016.

Tetsuya Mizumoto was awarded a Bachelor of Engineering degree in Electrical and Electronic Engineering in March 1979, and a Doctor of Engineering degree in Electrical and Electronic Engineering in March 1984, all from the Tokyo Institute of Technology (Tokyo Tech), Tokyo, Japan. He began working for Tokyo Tech in April 1984 as a research associate in the Faculty of Engineering and was promoted to full professor with the Graduate School of Engineering in April 2004. From October 2012 to March 2018, he served as Vice-President for Education at Tokyo Tech, and became Executive Vice-President for Education in April 2018. His research fields are applied optics, photonic circuits, and information and communication engineering. His research activity has been concerned mainly with waveguide optical devices, especially magneto-optic devices and all-optical switching devices based on the third-order nonlinearity. Dr. Mizumoto received the Treatise Award in 1994 and the Best Letter Award of Electronics Society Transactions in 2007 from the Institute of Electronics, Information and Communication Engineers (IEICE). He was awarded the Institute of Electrical and Electronics Engineers (IEEE) Photonics Society Distinguished Lecturer Awards in July 2009, IEEE Fellow grade in January 2012, and IEICE Achievement Award in May 2012. He is a fellow of IEICE, member of the Japan Society of Applied Physics, and the Magnetic Society of Japan.